A.O.Kaminsky[1], M.V.Dudyk[2], V.M.Fenkiv[2], Y.O.Chornoivan[1]

ON THE SCOPE AND LIMITATIONS OF THE COMNINOU MODEL FOR THE CRACK ON THE POLYGONAL INTERFACE

[1] S.P.Timoshenko Institute of Mechanics, National Academy of Sciences, Nesterov st., 3, 03057, Kyiv, Ukraine; e-mail:fract@inmech.kiev.ua
[2] Pavlo Tychyna Uman State Pedagogical University, Sadova st., 2, 20300, Uman, Cherkassy region, Ukraine; e-mail: dudik_m@hotmail.com

Abstract. A plane strain problem is investigated for the local stress and displacement fields near the angular point of the polygonal interface of two dissimilar homogeneous isotropic materials. It is supposed that the interface is weakened by an interface crack with the tip at the angular point. The contact zone near the crack tip is modeled by the cut with the frictional contact between faces according to the Comninou model. The asymptotic expressions for the components of displacement gradients and stress tensor near the crack tip are found using the Wieghardt-Williams method. A characteristic equation is obtained to determine the singularity order at the crack tip. A numerical analysis of the order of singularity dependence on the angle of the interface and the ratio of Young's moduli of the bounding materials is given. It is shown that the Comninou model can be used in this problem to get rid of the displacement oscillations near the angular point of the interface between two dissimilar materials. The obtained results are used to determine the scope of model applicability.

Key words: fracture, interface crack, polygonal interface, Wieghardt-Williams method, singularity order, contacting faces.

1. Introduction.

Solving many problems of fracture mechanics requires knowledge of the stress-strain state near various natural defects in the structure of solids and near the sharp technological elements of structures, which are a source of high-stress levels. When calculated within the framework of the linear elasticity theory, local stresses are singular in the vicinity of the concentrator vertices. The foundations of linear fracture mechanics were laid in the last century by A. Griffith, G. R. Irwin, E. Orowan. The fracture criteria formulated by them ensured significant progress in the mechanics of fracture, first of all, of homogeneous bodies with cracks.

The next step in the development of fracture mechanics was to take into account the influence of pre-fracture zones on the stress-strain state near the crack vertices. To this end, more complex models of cracked bodies have been developed, in particular, the models of Barenblatt [6] and Dugdale [17] and their generalization [9, 26 – 30], which provide a zone of pre-destruction by rupture lines.

At the same time, studies of piecewise homogeneous bodies with a crack at the flat interface between two dissimilar materials, carried out by Williams [42], Erdogan [20], England [19], Rice and Sih [37], and others, resulted in the physically impossible mutual intersection of crack edges due to spatial oscillations of displacement in the bound bodies near the vertices. Further investigations showed that oscillatory singularities at the tip of the opened interface crack cannot be vanished by taking into account additional factors, namely the curvilinear form of the interface crack [43], taking into account the spatial configuration of the piecewise homogeneous body [7] and anisotropy of the materials [36]. The oscillatory

singularity of the displacement field in the vicinity of the crack tip is an important issue in thermoelasticity [31] and piezoelectricity in bimaterials with impermeable and permeable interface crack [21].

Oscillating singularities at the tip of the opened interface crack caused some difficulties with the correct application of the linear fracture mechanics criteria [23]. A solution to this problem was proposed by M. Comninou [11]. It supposes a face contact area near the tip of the interface crack. Investigations by Comninou [10, 11], Comninou and Dundurs [12], Dundurs and Gautesen [18], Anderson [1], Y. A. Antipov et al. [3], Atkinson [4], Audoly [5], Leguillon [32] and others did confirm the elimination of displacement oscillations and the preservation of the power-law stress singularity due to the contacting faces for the planar interface between isotropic materials. The contact model was successfully used to investigate planar interfaces of various anisotropic, piezoelectric, electrically permeable, and dielectric materials in various configurations [21, 22, 24, 25, 39].

But is the Comninou model perfect? Does it guarantee that there will be no oscillatory singularity for every interface crack? In this paper, to answer this question we consider a crack in the piecewise linear interface. As was stated earlier, the vast majority of interface crack studies deal with the case when the crack is located on the planar interface between two dissimilar media. However, in the structure of modern industrial products or rocks, the appearance of interface cracks located at the broken interface is possible. Not enough attention has been paid to the determination of the stress-strain state in the vicinity of the vertices of such cracks. In particular, Theocaris and Gdoutos [38], using the Muschelishvili complex potential method, obtained explicitly characteristic equations for stress singularity orders within the first, second, and mixed basic problems of the theory of elasticity for an interface crack emerging from the angular point of two dissimilar homogeneous materials neglecting possible contact between the crack faces.

Under certain assumptions, the stress singularity orders under the above conditions can be determined from the results of local stress field studies in the vicinity of the common vertex of a multiwedge heterogeneous system [8, 13, 33–35]. In work [15], an analysis of the stress field near the tip of the open crack emerging from the angular point of the interface was performed. Following the results of Theocaris and Gdoutos [38], it is shown that in a rather wide range of fracture angles the stress singularity order is complex. As in the case of an interface crack at the planar interface, this yields spatial oscillations of the crack face displacement. As it was mentioned above, an alternative to the model of the open interface crack is the model of a crack with contacting faces (the Comninou model), in which, as in the model of M. Comninou, the displacement oscillation can be eliminated. In this regard, it is important to study the local field of stresses and displacements near the angular point of the boundary between two dissimilar materials, from which the interface crack emerges. The faces are supposed to interact according to the law of dry friction. The problem is to find the scope of model applicability and the asymptotic expressions for the components of the stress tensor near the crack tip under the conditions of plane strain. These asymptotic expressions can be used to determine the limiting states of piecewise homogeneous bodies with interface crack, the cohesive zone parameters at the crack tip, etc.

The general notation and the problem statement is given in Sect. 2. Section 3 is devoted to the solution of the problem. The solution and its implications are discussed in Sect. 4. The corresponding asymptotical near-tip stress field is analyzed in Sect. 5 with some necessary functions given in Appendix A.

2. Problem statement.

Consider the behavior of stresses near the tip of an interface crack under the plane strain condition. The tip of the crack is located in the angular point of the polygonal boundary between two dissimilar elastic homogeneous isotropic materials. The materials are characterized by Young's moduli E_1, E_2 and Poisson's ratios ν_1, ν_2, respectively. It is assumed that part of the crack faces of length s is in Coulomb frictional contact (Fig. 1). The coefficient of friction is μ. Following the general stress behavior near the angular points of elastic bodies (at distances $r \ll s$), we arrive at a homogeneous problem of elasticity theory for a piecewise homogeneous plane with a boundary between materials in

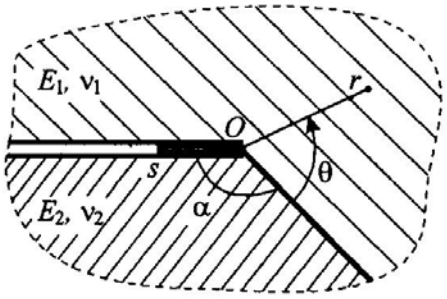

Fig. 1

the form of rectilinear sides of an angle. A half-infinite crack with contacting faces emerges from the angle vertex. Local structure of a piece-homogeneous body with an interface crack is depicted in Fig. 1.

In what follows the polar coordinate system (r,θ) is introduced in such way that the pole O is at the vertex of the angle of measure α on the interface and the polar axis is located along the bound line of materials. Taking into account the contact of the crack edges and the condition of continuity of stresses and displacements at the bound line of materials, one can formulate the boundary value problem of the theory of elasticity as follows:

$$\begin{gathered}
\sigma_\theta^1(r,0)=\sigma_\theta^2(r,0);\ \ \tau_{r\theta}^1(r,0)=\tau_{r\theta}^2(r,0);\\
u_\theta^1(r,0)=u_\theta^2(r,0);\ \ u_r^1(r,0)=u_r^2(r,0);\\
\sigma_\theta^1(r,\beta)=\sigma_\theta^2(r,-\alpha);\\
\tau_{r\theta}^1(r,\beta)=\tau_{r\theta}^2(r,-\alpha)=-\mu\sigma_\theta^1(r,\beta);\\
u_\theta^1(r,\beta)=u_\theta^2(r,-\alpha)\quad(\beta=2\pi-\alpha),
\end{gathered}\tag{1}$$

where superscripts denote the number of material, σ_r, σ_θ, $\tau_{r\theta}$ are the radial and tangential components of the stress tensor, and u_r, u_θ are components of the displacement vector.

3. Determination of stress singularity orders.

Since the studied body is a combination of two elastic wedges, we use the Wieghardt-Williams method [40, 41] to expand the solutions of the theory of elasticity equations by eigenfunctions and present the stresses and derivatives of displacements in each of the materials as

$$\begin{gathered}
\sigma_\theta^n(r,\theta)=r^\lambda[a_1^n\sin(\lambda+2)\theta+a_2^n\sin\lambda\theta+a_3^n\cos(\lambda+2)\theta+a_4^n\cos\lambda\theta];\\
\tau_{r\theta}^n(r,\theta)=-\frac{r^\lambda}{(\lambda+2)}[a_1^n(\lambda+2)\cos(\lambda+2)\theta+\\
+a_2^n\lambda\cos\lambda\theta-a_3^n(\lambda+2)\sin(\lambda+2)\theta-a_4^n\lambda\sin\lambda\theta];\\
\sigma_r^n(r,\theta)=-\frac{r^\lambda}{\lambda+2}[a_1^n(\lambda+2)\sin(\lambda+2)\theta+\\
+a_2^n(\lambda-2)\sin\lambda\theta+a_3^n(\lambda+2)\cos(\lambda+2)\theta+a_4^n(\lambda-2)\cos\lambda\theta];\\
\frac{\partial^2u_\theta^n(r,\theta)}{\partial r^2}=-\frac{1+\nu_n}{E_n}\frac{\lambda r^{\lambda-1}}{\lambda+2}[a_1^n(\lambda+2)\times\cos(\lambda+2)\theta+a_2^n(\lambda+4-4\nu_n)\cos\lambda\theta-\\
-a_3^n(\lambda+2)\sin(\lambda+2)\theta-a_4^n(\lambda+4-4\nu_n)\sin\lambda\theta];\\
\frac{\partial u_r^n(r,\theta)}{\partial r}=-\frac{1+\nu_n}{E_n}\frac{r^\lambda}{\lambda+2}[a_1^n(\lambda+2)\sin(\lambda+2)\theta+\\
+a_2^n(\lambda-2+4\nu_n)\sin\lambda\theta+a_3^n(\lambda+2)\cos(\lambda+2)\theta+a_4^n(\lambda-2+4\nu_n)\cos\lambda\theta];
\end{gathered}\tag{2}$$

$n=1$ for $0 \le \theta \le \beta$ and $n=2$ for $-\alpha \le \theta \le 0$. Satisfying the boundary conditions (1) using the Eqs. (2), we arrive at a system of linear homogeneous algebraic equations for the coefficients $a_j^n (j=1\ldots 4)$. For this system to have a nontrivial solution, its determinant should be zero. This condition leads to the characteristic equation of the problem for determining the exponent λ in the functional dependence of stresses from the distance r to the crack tip. After calculating the determinant and its algebraic transformations, this equation gives

$$D(\lambda)=0;\ D(\lambda)=D_1(\lambda)+\mu D_2(\lambda), \tag{3}$$

where

$$D_1(\lambda)=(1-e)[0,5(1+\kappa_1)D_{11}t_1-0,5e(1+\kappa_2)D_{12}t_3+e(1+\kappa_1)(1+\kappa_2)d_3]+$$
$$+e(1+\kappa_1)(1+\kappa_2)D_{13};$$
$$D_2(\lambda)=(1-e)\{(1+\kappa_1)D_{21}t_1-e(1+\kappa_2)[D_{22}t_3-(1+\kappa_1)d_4]+2(1-e)^2t_1t_3\}+$$
$$+e(1+\kappa_1)(1+\kappa_2)D_{23};$$
$$D_{11}(\lambda)=(1-e)d_5+(1+\kappa_1)\sin 2(\lambda+1)(2\pi-\alpha);$$
$$D_{12}(\lambda)=e(1+\kappa_2)\sin 2(\lambda+1)\alpha+(1-e)d_2;$$
$$D_{13}(\lambda)=\sin^2\lambda\pi[(1+\kappa_1)d_7-e(1+\kappa_2)d_9];$$
$$D_{21}(\lambda)=(1-e)d_6-(1+\kappa_1)t_2;$$
$$D_{22}(\lambda)=e(1+\kappa_2)t_4+(1-e)d_1;$$
$$D_{23}(\lambda)=\sin^2\lambda\pi[(1+\kappa_1)-e(1+\kappa_2)]d_8;$$
$$d_1=(\lambda+1)\sin^2\alpha+3t_4;\ d_2=(\lambda+1)\sin 2\alpha+\sin 2(\lambda+1)\alpha;$$
$$d_3=\left[(\lambda+1)^2\sin^2\alpha+\sin(\lambda+1)\alpha\sin(\lambda+1)\beta\right]\sin 2(\lambda+1)(\alpha-\pi)-$$
$$-2(\lambda+1)\sin^2\lambda\pi\sin 2\alpha\cos^2(\lambda+1)(\pi-\alpha);$$
$$d_4=2\left[(\lambda+1)^2\sin^2\alpha+\sin(\lambda+1)\alpha\sin(\lambda+1)\beta\right]\sin^2(\lambda+1)(\pi-\alpha)-$$
$$-4\sin^2\lambda\pi\left[(\lambda+1)\sin^2\alpha\cos^2(\lambda+1)(\pi-\alpha)+\sin(\lambda+1)\alpha\sin(\lambda+1)\beta\right];$$
$$d_5=(\lambda+1)\sin 2\alpha-\sin 2(\lambda+1)\beta;\ d_6=(\lambda+1)\sin^2\alpha+3t_2;$$
$$d_7=(\lambda+1)\sin\alpha\cos\alpha-\sin(\lambda+1)\alpha\cos(\lambda+1)\beta;$$
$$d_8=(\lambda+1)\sin^2\alpha+\sin(\lambda+1)\alpha\sin(\lambda+1)\beta;$$
$$d_9=(\lambda+1)\sin\alpha\cos\alpha+\cos(\lambda+1)\alpha\sin(\lambda+1)\beta;$$
$$t_1=(\lambda+1)^2\sin^2\alpha-\sin^2(\lambda+1)\alpha;\ t_2=\sin^2(\lambda+1)\beta;$$
$$t_3=(\lambda+1)^2\sin^2\alpha-\sin^2(\lambda+1)\beta;\ t_4=\sin^2(\lambda+1)\alpha;$$
$$e=\frac{E_1}{E_2}\frac{1+\nu_2}{1+\nu_1};\ \kappa_{1(2)}=3-4\nu_{1(2)}.$$

When $\alpha=\pi$, Eq. (3) can be reduced to the known result by Comninou [11]

$$\cos\lambda\pi + \mu\beta_D \sin\lambda\pi = 0;\ \ \beta_D = \frac{(1+e\kappa_2)-(e+\kappa_1)}{(1+e\kappa_2)+(e+\kappa_1)},$$

where β_D is the so-called «second Dundurs' parameter». The corresponding order of the stress singularity in this case is $\lambda = -\pi^{-1}\operatorname{arccot}|\mu\beta_D|$.

4. The contact model implications and its scope of applicability.

It follows from (2) that the stress behavior near the crack tip will be singular if Eq. (3) has roots in the range $-1 < \mathrm{Re}\lambda < 0$ (roots with $\mathrm{Re}\lambda \le -1$ are inacceptable as they yield infinite displacements for $r \to 0$). If the root with the smallest real part, say λ_1, is real then we have a simple power-law singularity. However, if λ_1 has a non-zero imaginary part then we have a power-law singularity $\mathrm{Re}\lambda_1 < 0$ with oscillations along the radial coordinate. This gives us stresses as $\sigma_{ik} \sim r^{Re\lambda_1}\cos(\mathrm{Im}\lambda_1 \cdot \ln r + \varphi)$ (φ is a constant). A similar oscillating factor in a formula for displacements gives an unphysical crack face penetration.

The results below are given for the stress state near the crack tip for Young's moduli that meet the condition $E_1 < E_2$. The obtained conclusions can be transferred to the case of $E_1 > E_2$ by the simultaneous substitutions $E_1 \leftrightarrow E_2$, $\nu_1 \leftrightarrow \nu_2$, $\mu \to -\mu$, $\alpha \to 2\pi - \alpha$.

Numerical analysis of equation (3) reveals that there can be 1 or 2 of such roots. Fig. 2, *a* shows the dependencies of the singularity orders λ_1, λ_2 for $E_1 / E_2 = 0{,}1$, $\nu_1 = \nu_2 = 0{,}3$ for $\mu = 0$ (solid line), $\mu = 2$ (dashed line) and $\mu = -2$ (dot-dashed line); the sign of μ is determined by the direction of relative shear displacement of the crack faces. This displacement also determines the contact zone extent.

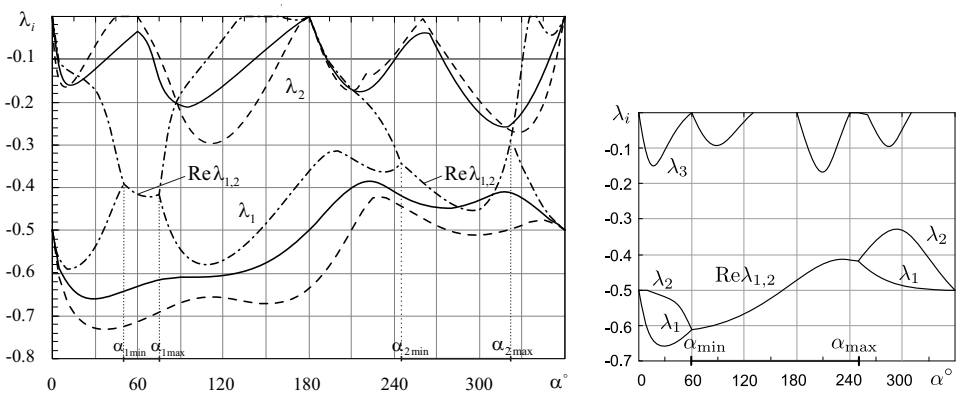

a *b*

Fig. 2

The last statement is a conclusion of the contact interface crack studies for the linear interfaces by Dundurs and Gautesen [18]. In what follows, the study is focussed on configurations with $E_1 < E_2$ and $\mu < 0$ (Fig. 1). This parameter combination corresponds to the case of substantial contact zone extent.

As it is shown in works [15, 38], the singularity order near the tip of the open interface crack has a non-zero imaginary part at certain ranges of bending angles ($\alpha_{1\min}$, $\alpha_{1\max}$) (the area in Fig. 2, *b* denoted as $\mathrm{Re}\lambda_{1,2}$). This leads to unphysical oscillatory behavior. Due to the contacting crack faces for $\mu \ge 0$ (Fig. 2, *a*), solid and dashed lines) the order of singularity λ_1 becomes a purely real number for an arbitrary bending angle, hence the stresses have a power-law singularity and there is no oscillatory behavior near the crack tip. Thus,

the Comninou model for $\mu \geq 0$, $E_1 / E_2 < 1$ allows to avoid the shortcomings of the classical model of open interface crack.

However, for $\mu < 0$ at certain ranges of bending angles ($\alpha_{1\min}$, $\alpha_{1\max}$), which depend on the ratio of Young's moduli of the bound materials and the coefficient of friction (Table), the singularity orders can reach complex conjugate values $\lambda_1 = \overline{\lambda}_2$, which cause physically incorrect spatial displacement oscillations (dash-dotted line, range $\mathrm{Re}\lambda_{1,2}$ on the plot for $\mu = -2$, Fig. 2, *a*). Thus, the Comninou model becomes ineffective for the bending angles from this range.

Table

E_1 / E_2	0,1		0,3		0,5		0,7		0,9	
μ	–1	–2	–1	–2	–1	–2	–3	–4	–12	–13
$(\alpha_{1\min}, \alpha_{1\max})$	–	(46, 77)	–	(57, 84)	–	(55, 91)	–	(73, 76)	–	(64, 84)
$(\alpha_{2\min}, \alpha_{2\max})$	(264, 317)	(242, 322)	(274, 305)	(252, 312)	(267, 305)	(267, 305)	–	(268, 304)	(277, 296)	(272, 300)
$(\alpha_{\min}, \alpha_{\max})$	(61, 252)		(75, 258)		(82, 262)		(86, 266)		(89, 268)	

The width of the intervals ($\alpha_{1\min}$, $\alpha_{1\max}$) and ($\alpha_{2\min}$, $\alpha_{2\max}$) depends on the ratio of Young's moduli of the bound materials and the coefficient of friction and tends to zero as the elastic characteristics of the materials becomes closer and the coefficient of friction decreases (Table). The corresponding range of the bending angles for the open crack is given in Table as values $\alpha_{\min}$, $\alpha_{\max}$. If the coefficient of friction allows the existence of ($\alpha_{1\min}$; $\alpha_{1\max}$), ($\alpha_{2\min}$; $\alpha_{2\max}$) for the model with contacting faces, these intervals are substantially narrower than the interval ($\alpha_{\min}$; $\alpha_{\max}$).

Dependence of the stress singularity order near the tip of the interface crack with contacting (a) and load-free (b) faces on the bending angle of the interface [15, 38] for $E_1 / E_2 = 0{,}1$, $\nu_1 = \nu_2 = 0{,}3$ is shown in Fig. 2.

The ranges of bending angles of the interface (in degrees), which correspond to the complex orders of the singularity at the tip of the interface crack with the contacting faces ($\nu_1 = \nu_2 = 0{,}3$) are given in Table.

For every couple of the interface parameter values (E_1 / E_2, α), there exists a limiting value of the coefficient of friction μ_c such that the order of singularity has a non-zero imaginary part for $\mu < \mu_c$ ($|\mu| > |\mu_c|$) (Fig. 3). The closer Young's moduli of the bound materials to each other, the bigger is $|\mu_c|$.

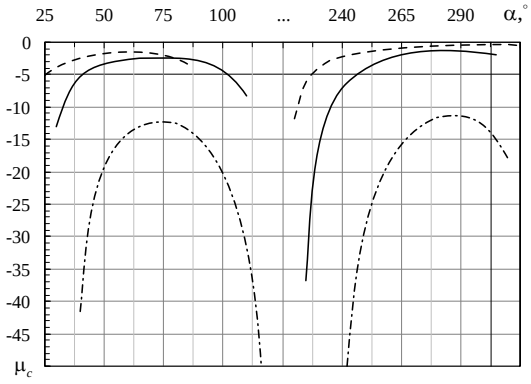

Fig. 3

The dependence of the stress singularity order near the tip of the interface crack on the coefficient of friction for the bending angles $\alpha = 200^\circ$ (a) and $\alpha = 300^\circ$ (b) ($\nu_1 = \nu_2 = 0{,}3$; dashed line is for $E_1 / E_2 = 0{,}1$, solid line is for $E_1 / E_2 = 0{,}5$, dash-dotted line is for $E_1 / E_2 = 0{,}9$ is shown in Fig. 4.

As it can be seen from the comparison of Figs. 2, *a* and 2, *b*, the singularity orders λ_1 near the tip of the crack with contacting faces and the open crack for most values of the interface bending angles are close to each other and to the value of $-0{,}5$, which

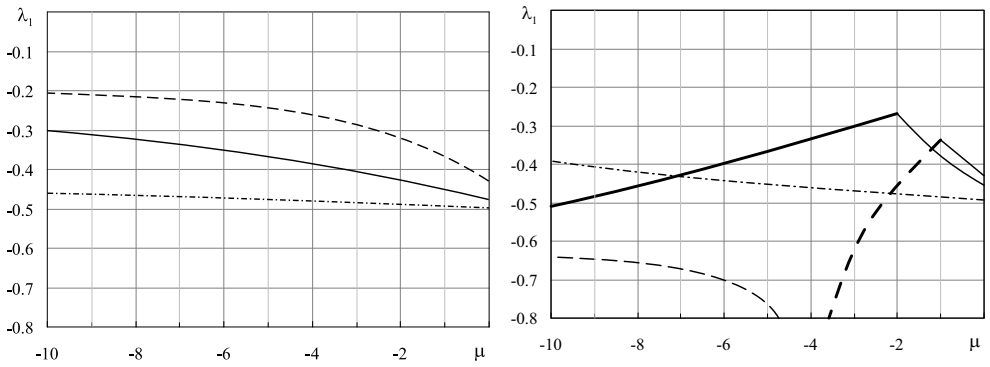

a *b*

Fig. 4

corresponds to a crack in a homogeneous body. At the same time, the values of λ_2 differ quite signi-ficantly, so according to their values, the effect of λ_2 on the stress state near the tip in the case of a closed crack is assumed to be much smaller than for the open one. According to our calculations (Fig. 4) the friction escalation ($\mu' < \mu'' < 0$) leads to the decrease of the stress concentration ($\lambda_1' > \lambda_1''$). This pattern does not hold for the complex orders of singu-larity (Fig. 4, *b*, bolder lines on the plot). The corresponding ranges of parameters should be treated according to other models of interface crack.

The limiting values of the coefficient of friction for various bending angles are shown in Fig. 3 ($\nu_1 = \nu_2 = 0{,}3$; dashed line is for $E_1 / E_2 = 0{,}1$, solid line is for $E_1 / E_2 = 0{,}5$, dash-dotted line is for $E_1 / E_2 = 0.9$).

5. Asymptotical near-tip stress field.

Consider one of the coefficients a_j^n for each of the found roots λ_i of Eq. (3) to be known and equal to a given constant, namely: $a_4^2(\lambda_i) = C_i$. This allows us to determine the remaining coefficients, expressing them in C_i , and obtain the desired formulas for the local field of stresses and displacements near the crack tip, which are given as a superposition of partial solutions of the problem with $\operatorname{Re}\lambda_i > -1$:

$$\sigma_\theta(r,\theta) = \sum_i C_i F_1(\lambda_i,\theta) r^{\lambda_i};\ \tau_{r\theta}(r,\theta) = \sum_i C_i F_2(\lambda_i,\theta) r^{\lambda_i};$$

$$\sigma_r(r,\theta) = \sum_i C_i F_3(\lambda_i,\theta) r^{\lambda_i};$$

$$\frac{\partial^2 u_\theta(r,\theta)}{\partial r^2} = \sum_i C_i F_4(\lambda_i,\theta) r^{\lambda_i - 1};\ \frac{\partial u_r(r,\theta)}{\partial r} = \sum_i C_i F_5(\lambda_i,\theta) r^{\lambda_i};$$

$$F_m(\lambda,\theta) = \begin{cases} F_m^1(\lambda,\theta), & 0 \le \theta \le 2\pi - \alpha, \\ F_m^2(\lambda,\theta), & -\alpha \le \theta \le 0; \end{cases} \quad (m = 1\ldots5)$$

$$F_1^n(\lambda,\theta) = \tilde{a}_1^n(\lambda)\sin(\lambda+2)\theta + \tilde{a}_2^n(\lambda)\sin\lambda\theta + \tilde{a}_3^n(\lambda)\cos(\lambda+2)\theta + \tilde{a}_4^n(\lambda)\cos\lambda\theta;$$

$$F_2^n(\lambda,\theta) = -\tilde{a}_1^n(\lambda)\cos(\lambda+2)\theta - \tilde{a}_2^n(\lambda)\frac{\lambda}{\lambda+2}\cos\lambda\theta + \tilde{a}_3^n(\lambda)\sin(\lambda+2)\theta +$$

$$+\tilde{a}_4^n(\lambda)\frac{\lambda}{\lambda+2}\sin\lambda\theta;$$

$$F_3^n(\lambda,\theta) = -\Big[\tilde{a}_1^n(\lambda)\sin(\lambda+2)\theta + \tilde{a}_2^n(\lambda)\frac{\lambda-2}{\lambda+2}\sin\lambda\theta + \tilde{a}_3^n(\lambda)\cos(\lambda+2)\theta + \\ + \tilde{a}_4^n(\lambda)\frac{\lambda-2}{\lambda+2}\cos\lambda\theta\Big]; \quad (4)$$

$$F_4^n(\lambda,\theta) = -\frac{1+\nu_n}{E_n}\frac{\lambda}{\lambda+2}\Big[\tilde{a}_1^n(\lambda)(\lambda+2)\cos(\lambda+2)\theta + \tilde{a}_2^n(\lambda)(\lambda+4-4\nu_n)\cos\lambda\theta - \\ -\tilde{a}_3^n(\lambda)(\lambda+2)\sin(\lambda+2)\theta - \tilde{a}_4^n(\lambda)(\lambda+4-4\nu_n)\sin\lambda\theta\Big];$$

$$F_5^n(r,\theta) = -\frac{1+\nu_n}{E_n(\lambda+2)}[\tilde{a}_1^n(\lambda)(\lambda+2)\sin(\lambda+2)\theta + \tilde{a}_2^n(\lambda)(\lambda-2+4\nu_n)\sin\lambda\theta + \\ +\tilde{a}_3^n(\lambda)(\lambda+2)\cos(\lambda+2)\theta + \tilde{a}_4^n(\lambda)(\lambda-2+4\nu_n)\cos\lambda\theta].$$

The functions $\tilde{a}_j^n(\lambda)$ are given in Appendix A. Thus, the Eqs. (4) up to C_i constants, which depend on the geometry of piecewise homogeneous body and applied loads, completely determine the field of stresses and displacements around the angular point of the materials interface. The quotients C_i take into account the external load and the structure of a specific piecewise homogeneous body but they cannot be determined in the framework of Wieghardt-Williams method and should be obtained numerically.

The main terms of the expansion (4) correspond to the smallest singularity order in the $-1 < \mathrm{Re}\lambda < 0$ strip, say λ_1. These terms determine the stressed state in the vicinity of the crack tip. Taking this into account, the factor C_1 is subject to the condition $C_1 F_1(\lambda_1, -\alpha) < 0$, which corresponds to the compressive normal stress on the crack faces and ensures their contact.

The angular distribution of stress and strain in the crack tip is determined by the functions $F_m(\lambda_1,\theta)$. The dependence of the normal ($\sigma_\theta \sim F_1(\lambda_1,\theta)$) and tangential ($\tau_{r\theta} \sim F_2(\lambda_1,\theta)$) stresses on the polar angle in the coordinate system depicted in Fig. 1 is shown in Fig. 5 for $\alpha = 200^\circ$, $E_1/E_2 = 0.1$, $\nu_1 = \nu_2 = 0{,}3$, $\mu = -2$. According to this figure, $F_1(\lambda_1, -\alpha) < 0$. Thus, the crack face contact implies $C_1 > 0$.

Angles for the extremal values of the nor-mal and tensile stresses, denoted θ_m here, can be found from the angular dependency of the stresses. These angles can be used to obtain esti-mations of the primal initial directions of (small-scale) prefracture zones. As a consequence one can evaluate possible directions of the crack propagation. In particular, if it is the brittle crack that propagates due to the tensile deformations then the propagation direction angle θ_1 can be determined from the condition of the maximum value of $F_1(\lambda_1,\theta_1)$. For the example in Fig. 5, this gives us $\theta_1 \approx 46^\circ$. For the ductile materials, the initial plastic zone orientation can be approximately determined from the condition of $F_2(\lambda_1,\theta_2)$ maximum value. For the example in Fig. 5, $\theta_1 \approx 46^\circ$ for the first material and $\theta_2 \approx -139^\circ$ for the second material.

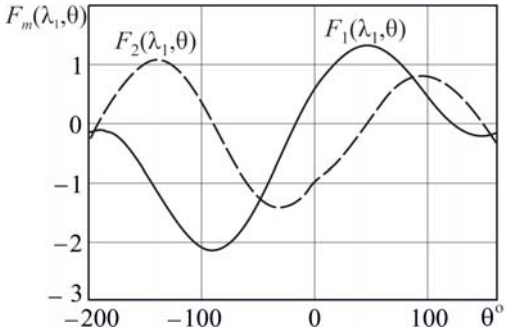

Fig. 5

The obtained solution allows us to estimate the length of the contact area of the faces using the distance from the tip to the point where the normal stress on the faces of the crack are equal to zero. Limiting the expansion of $\sigma_\theta(r, 2\pi-\alpha)$ to the first two terms, one can find that

$$s \approx L\left(-n\frac{F_1(\lambda_1, 2\pi-\alpha)}{F_2(\lambda_2, 2\pi-\alpha)}\right)^{1/(\lambda_2-\lambda_1)}. \quad (5)$$

where $n = (C_1 L^{\lambda_1})/(C_2 L^{\lambda_2})$ is the dimensionless parameter which depends on the configuration of the piecewise homogeneous body and external loading. Since the found solution takes into account the local stress field, the use of the obtained contact zone length estimate is limited by the requirement that the zone dimensions should be much smaller than the crack length or any other governing lengths (distances from crack tip to nearest body boundary, to the nearest point of external forces application, etc.). For example, the assessment of the contact zone length is physically valid, $s \approx 0{,}005L$, for $n = 0{,}01$ and $\alpha = 200^\circ$, $E_1 / E_2 = 0{,}1$, $\nu_1 = \nu_2 = 0{,}3$, but $n = 0{,}05$ yields an invalid value $s \approx 1{,}395L > L$.

It is worth noting that the contact zone length in approximation from Eq. (5) does not change for the simple loading as C_1 / C_2 in n does not change with proportional growth of the stress components. This conclusion is in agreement with the results of the contact model of crack for flat interfaces [4, 12, 18].

6. Conclusions.

Knowing how stress and displacement are distributed near the crack tip is important to evaluate the strength of the solids. The results of this work can be of use for designers and engineers to evaluate parameters of limiting states of the piecewise homogeneous bodies with polygonal interface. The results for the interface crack at the flat interface have been already obtained a relatively long time ago. This work initiates investigations for the general case of the crack at the polygonal interface. The local stress and displacement fields found in this work as well as the corresponding orders of the stress singularity at the tip of the interface crack emerging from the interface angular point can be used to make the industrial designs physically and mathematically valid.

The expressions found for stress and displacement fields near the interface crack tip can also be used in fracture mechanics to study the parameters of small-scale cohesive zones and limiting loads in piecewise homogeneous bodies with a polygonal interface. This problem is partially solved for the case of an open crack [15], but it remains unsolved for the case of a crack with contacting faces.

Besides of the practical applications, an important corrolary of this work lies in analysis of the theoretical basics of solving the interfcae crack problem. It is found that the modeling of interface cracks emerging from the angular point of the interface using Coulomb's friction law and taking into account the face contact can be used to get rid of spatial oscillations of face displacement, which are inevitable when using the model of open interface crack. However, it is shown that the crack model of the Comninou type with contacting faces still can have small intervals of interface bending angles, for which, depending on the direction of shear displacement of the crack faces, there are also complex singularity orders responsible for oscillations of face displacements.

Hence, the interface crack model with contacting faces does not give the universal solution to the problem of oscillatory singularity elimination. We believe that this problem can be solved by introducing a prefracture zone near the crack tip. This is the essence of the complex interface crack model [16, 30]. It should be mentioned that unphysical displacement oscillations can also be eliminated by introducing other features into the vicinity of the crack tip, namely the crack face cohesion without sliding [14], unideal material conjuction [2], etc.

Appendix A. Eigen functions in expansions of the stresses and displacement derivatives near the interface crack tip for the case of the crack faces contact.

$$\tilde{a}_1^2(\lambda) = \Delta_{12}(\lambda)B_1(\lambda) - \Delta_{22}(\lambda)B_2(\lambda) + \Delta_{32}(\lambda)B_3(\lambda);$$

$$\tilde{a}_2^2(\lambda) = -\Delta_{11}(\lambda)B_1(\lambda) + \Delta_{21}(\lambda)B_2(\lambda) - \Delta_{31}(\lambda)B_3(\lambda);$$

$$\tilde{a}_3^2(\lambda) = \Delta_{14}(\lambda)B_4(\lambda) + \Delta_{24}(\lambda)B_5(\lambda) + \Delta_{34}(\lambda)B_6(\lambda);$$

$$\tilde{a}_4^2(\lambda) = -\big(\Delta_{13}(\lambda)B_4(\lambda) + \Delta_{23}(\lambda)B_5(\lambda) + \Delta_{33}(\lambda)B_6(\lambda)\big);$$

$$\tilde{a}_1^1(\lambda) = \frac{1}{(1+\kappa_1)}\Big[\tilde{a}_1^2(\lambda)\big((1+\kappa_1) + \lambda(1-e)\big) +$$

$$+\tilde{a}_2^2(\lambda)\frac{\lambda}{\lambda+2}\big((1+\kappa_1) + \lambda(1-e) - e(1+\kappa_2)\big)\Big];$$

$$\tilde{a}_2^1(\lambda) = \frac{1}{(1+\kappa_1)}\Big[-\tilde{a}_1^2(\lambda)(\lambda+2)(1-e) - \tilde{a}_2^2(\lambda)\big(\lambda(1-e) - e(1+\kappa_2)\big)\Big];$$

$$\tilde{a}_3^1(\lambda) = \frac{1}{(1+\kappa_1)}\Big[\tilde{a}_3^2(\lambda)\big((1+\kappa_1) - (\lambda+2)(1-e)\big) +$$

$$+\tilde{a}_4^2(\lambda)\big((1+\kappa_1) - (\lambda+2)(1-e) - e(1+\kappa_2)\big)\Big];$$

$$\tilde{a}_4^1(\lambda) = \frac{1}{(1+\kappa_1)}\Big[\tilde{a}_3^2(\lambda)(\lambda+2)(1-e) + \tilde{a}_4^2(\lambda)\big((\lambda+2)(1-e) + e(1+\kappa_2)\big)\Big];$$

$$\Delta_{11}(\lambda) = (\lambda+2)\big[\cos(\lambda+2)\alpha + \mu\sin(\lambda+2)\alpha\big];$$

$$\Delta_{12}(\lambda) = \lambda\cos\lambda\alpha + \mu(\lambda+2)\sin\lambda\alpha;$$

$$\Delta_{13}(\lambda) = (\lambda+2)\big[\sin(\lambda+2)\alpha - \mu\cos(\lambda+2)\alpha\big];$$

$$\Delta_{14}(\lambda) = \lambda\sin\lambda\alpha - \mu(\lambda+2)\cos\lambda\alpha;$$

$$\Delta_{21}(\lambda) = (1-e)(\lambda+2)\big[\cos\lambda\beta - \cos(\lambda+2)\alpha\big];$$

$$\Delta_{22}(\lambda) = \big[\lambda(1-e) - e(1+\kappa_2)\big]\big(\cos\lambda\beta - \cos\lambda\alpha\big);$$

$$\Delta_{23}(\lambda) = (1-e)(\lambda+2)\big[\sin\lambda\beta - \sin(\lambda+2)\alpha\big];$$

$$\Delta_{24}(\lambda) = (1-e)\big[(\lambda+2)\sin\lambda\beta - \lambda\sin\lambda\alpha\big] + e(1+\kappa_2)\big(\sin\lambda\alpha + \sin\lambda\beta\big);$$

$$\Delta_{31}(\lambda) = (1-e)\delta_{11}(\lambda) + (1+\kappa_1)\big[\sin(\lambda+2)\beta + \sin(\lambda+2)\alpha\big];$$

$$\Delta_{32}(\lambda) = \frac{(1-e)\lambda - e(1+\kappa_2)}{\lambda+2}\delta_{11}(\lambda) + \frac{1+\kappa_1}{\lambda+2}\big[\lambda\sin(\lambda+2)\beta + (\lambda+2)\sin\lambda\alpha\big];$$

$$\Delta_{33}(\lambda) = (1-e)(\lambda+2)\delta_{12}(\lambda) + (1+\kappa_1)\big[\cos(\lambda+2)\beta - \cos(\lambda+2)\alpha\big];$$

$$\Delta_{34}(\lambda)=\left[(\lambda+2)(1-e)+e(1+\kappa_2)\right]\delta_{12}(\lambda)+(1+\kappa_1)\left[\cos(\lambda+2)\beta-\cos\lambda\alpha\right];$$

$$B_1(\lambda)=(1-e)^2 B_{11}(\lambda)-e(1+\kappa_2)(1-e)B_{12}(\lambda)+(1+\kappa_1)(1-e)B_{13}(\lambda)-$$

$$-e(1+\kappa_2)(1+\kappa_1)B_{14}(\lambda);$$

$$B_{11}(\lambda)=-(\lambda+2)\delta_{12}(\lambda)\delta_{13}(\lambda);\ \ B_{12}(\lambda)=(\lambda+2)\left[\sin\lambda\alpha+\sin(\lambda+2)\alpha\right]\delta_{12}(\lambda);$$

$$B_{13}(\lambda)=-\left[(\lambda+2)\sin\lambda\beta\delta_{22}(\lambda)+\cos(\lambda+2)\beta\delta_{23}(\lambda)\right]+\delta_{32}(\lambda);$$

$$B_{14}(\lambda)=(\sin\lambda\alpha+\sin\lambda\beta)\left[\cos(\lambda+2)\beta-\cos(\lambda+2)\alpha\right];$$

$$B_2(\lambda)=(1-e)B_{21}(\lambda)+e(1+\kappa_2)B_{22}(\lambda)+(1+\kappa_1)B_{23}(\lambda);$$

$$B_{21}(\lambda)=(\lambda+2)\left[\delta_{23}(\lambda)+\mu(\lambda+2)\delta_{22}(\lambda)\right]\delta_{12}(\lambda);$$

$$B_{22}(\lambda)=(\lambda+2)\left[\sin(\lambda+2)\alpha-\mu\cos(\lambda+2)\alpha\right]\delta_{12}(\lambda);$$

$$B_{23}(\lambda)=\left[\delta_{23}(\lambda)+\mu(\lambda+2)\delta_{22}(\lambda)\right]\cos(\lambda+2)\beta-\delta_{32}(\lambda);$$

$$B_3(\lambda)=(1-e)B_{31}(\lambda)+e(1+\kappa_2)B_{32}(\lambda);$$

$$B_{31}(\lambda)=(\lambda+2)\left[\left[\delta_{32}(\lambda)+\mu(\lambda+2)\delta_{22}(\lambda)\right]\sin\lambda\beta-\mu\delta_{32}(\lambda)\right];$$

$$B_{32}(\lambda)=(\lambda+2)(\sin\lambda\beta+\sin\lambda\alpha)\left[\sin(\lambda+2)\alpha-\mu\cos(\lambda+2)\alpha\right];$$

$$B_4(\lambda)=(1-e)\left[\left[(1-e)\lambda-e(1+\kappa_2)\right]B_{41}(\lambda)+(1+\kappa_1)B_{42}(\lambda)\right]+$$

$$+e(1+\kappa_2)(1+\kappa_1)B_{43}(\lambda);$$

$$B_{41}(\lambda)=\delta_{11}(\lambda)\delta_{22}(\lambda);\ \ B_{42}(\lambda)=\lambda\sin(\lambda+2)\beta\delta_{22}(\lambda)-\cos\lambda\beta\delta_{21}(\lambda)-\delta_{31}(\lambda);$$

$$B_{43}(\lambda)=\left[\sin(\lambda+2)\alpha+\sin(\lambda+2)\beta\right](\cos\lambda\beta-\cos\lambda\alpha);$$

$$B_5(\lambda)=(1-e)B_{51}(\lambda)+e(1+\kappa_2)B_{52}(\lambda)+(1+\kappa_1)B_{53}(\lambda);$$

$$B_{51}(\lambda)=\left[\lambda\delta_{22}(\lambda)-\mu\delta_{21}(\lambda)\right]\delta_{11}(\lambda);$$

$$B_{52}(\lambda)=\left[\cos(\lambda+2)\alpha+\mu\sin(\lambda+2)\alpha\right]\delta_{11}(\lambda);$$

$$B_{53}(\lambda)=\left[\lambda\delta_{22}(\lambda)-\mu\delta_{21}(\lambda)\right]\sin(\lambda+2)\beta-\delta_{31}(\lambda);$$

$$B_6(\lambda)=(1-e)B_{61}(\lambda)-e(1+\kappa_2)B_{62}(\lambda);$$

$$B_{61}(\lambda)=(\lambda+2)\left[-\left[\lambda\delta_{22}(\lambda)-\mu\delta_{21}(\lambda)\right]\cos\lambda\beta+\mu\delta_{31}(\lambda)\right];$$

$$B_{62}(\lambda)=(\lambda+2)(\cos\lambda\beta-\cos\lambda\alpha)\left[\cos(\lambda+2)\alpha+\mu\sin(\lambda+2)\alpha\right];$$

$$\delta_{11}(\lambda)=\lambda\sin(\lambda+2)\beta-(\lambda+2)\sin\lambda\beta;\ \ \delta_{12}(\lambda)=\cos\lambda\beta-\cos(\lambda+2)\beta;$$

$$\delta_{13}(\lambda)=(\lambda+2)\sin(\lambda+2)\beta-\lambda\sin\lambda\beta;$$

$$\delta_{21}(\lambda)=\lambda\sin(\lambda+2)\alpha-(\lambda+2)\sin\lambda\alpha;\ \ \delta_{22}(\lambda)=\cos\lambda\alpha-\cos(\lambda+2)\alpha;$$

$$\delta_{23}(\lambda) = (\lambda+2)\sin(\lambda+2)\alpha - \lambda\sin\lambda\alpha;$$

$$\delta_{31}(\lambda) = -(\lambda+1)\sin 2\alpha + \sin 2(\lambda+1)\alpha;$$

$$\delta_{32}(\lambda) = (\lambda+1)\sin 2\alpha + \sin 2(\lambda+1)\alpha.$$

РЕЗЮМЕ. Досліджується локальне поле напружень і переміщень в умовах плоскої деформації біля кутової точки ламаної межі розділу двох різних однорідних ізотропних матеріалів. На одній із сторін межі розділу розташована тріщина, вершина якої збігається з точкою зламу. В рамках моделі М. Комніноу тріщина вважається математичним розрізом, береги якого контактують з тертям. За допомогою методу Віггардта – Вільямса розкладу розв'язків рівнянь теорії пружності за власними функціями знайдено асимптотичні вирази для компонент градієнтів переміщень та тензора напружень біля вершини тріщини. Чисельно проаналізовані залежності показників сингулярності від кута зламу межі розділу і відношення модулів Юнга з'єднаних матеріалів. Розраховано і обґрунтовано області можливого застосування моделі Комніноу, яка дозволяє усунути фізично неможливі просторові осциляції переміщень берегів тріщини біля кутової точки ламаної межі розділу двох різних матеріалів.

КЛЮЧОВІ СЛОВА: руйнування, міжфазна тріщина, кусково-лінійна межа розділу.

1. *Anderson P.M.* Small scale contact conditions for the linear-elastic interface crack // J. Appl. Mech. – 1988. – **55,** N 4. – P. 814 – 817.
2. *Antipov Y., Avila-Pozos O., Kolaczkowski S., Movchan A.* Mathematical model of delamination cracks on imperfect interfaces // Int. J. Solids Struct. – 2001. – **38,** N 36. – P. 6665 – 6697.
3. *Antipov Y., Bardzokas D., Exadaktylos G.* Interface edge crack in a bimaterial elastic half-plane // Int. J. Fract. – 1997. – **88** N 3. – P. 281 – 304.
4. *Atkinson C.* The interface crack with a contact zone (an analytical treatment) // Int. J. Fract. – 1982. – **18,** N 3. – P. 161 – 177.
5. *Audoly B.* Asymptotic study of the interfacial crack with friction // J. Mech. Phys. Solids. – 2000. – **48,** N 9. – P. 1851 – 1864.
6. *Barenblatt G.I.* On equilibrium cracks formed in brittle fracture. General concepts and hypotheses. Axisymmetric cracks // J. Appl. Mathem. Mech. – 1959. – **23,** N 3. – P. 622 – 636.
7. *Bercial-Velez J., Antipov Y., Movchan A.* High-order asymptotics and perturbation problems for 3D interfacial cracks // J. Mech. Phys. Solids. – 2005. – **53,** N 5. – P. 1128 – 1162.
8. *Carpinteri A., Paggi M.* Analytical study of the singularities arising at multi-material interfaces in 2D linear elastic problems // Engng. Fract. Mech. – 2007. – **74,** N 1. – P. 59 – 74.
9. *Cherepanov G.P.* Plastic rupture lines at the tip of a crack // J. Appl. Mathem. Mech. –1976. – **40,** N 4. – P. 666 – 674.
10. *Comninou M.* Interface crack with friction in the contact zone // J. Appl. Mech. – 1977. – **44,** N 4. – P. 780 – 781.
11. *Comninou M.* The interface crack // J. Appl. Mech. – 1977. – **44,** N 4. – P. 631 – 636.
12. *Comninou M., Dundurs J.* Effect of friction on the interface crack loaded in shear // J. Elasticity. – 1980. – **10,** N 2. – P. 203 – 212.
13. *Djoković J.M., Nikolić R.R., Ulewicz R., Hadzima B.* Interface crack approaching a three-material joint // Appl. Sci. – 2020. – **10,** N 1, P. 416 – 428.
14. *Dorogoy A., Banks-Sills L.* Effect of crack face contact and friction on Brazilian disk specimens – A finite difference solution // Engng. Fract. Mech. – 2005. – **72,** N 18. – P. 2758 – 2773.
15. *Dudyk M.V., Dikhtyarenko Y.V.* Development of a prefracture zone from an interface crack at a corner point of an interface of two elastic media // J. Mathem. Sci. – 2021. – **184,** N 2. – P. 121 – 135.
16. *Dudyk M.V., Kipnis L.A.* Model of the structure of the near tip area of interface crack in a piece-homogeneous elastic-plastic body // Strength, Fracture and Complexity. – 2018. – **11**. – P. 31 – 50.
17. *Dugdale D.S.* Yielding of steel sheets containing slits // J. Mech. Phys. Solids – 1960. – **8**. – P. 100 – 104.
18. *Dundurs J., Gautesen A.K.* An opportunistic analysis of the interface crack // Int. J. Fract. – 1988. – **36,** N 2. – P. 151 – 159.
19. *England A.H.* A crack between dissimilar media // J. Appl. Mech. – 1965. – **32,** N 2. – P. 400 – 402.
20. *Erdogan F.* Stress distribution in bonded dissimilar materials with cracks // J. Appl. Mech. – 1965. – **32,** N 2. – P. 403 – 410.

21. *Govorukha V., Kamlah M., Loboda V., Lapusta Y.* Fracture Mechanics of Piezoelectric Solids with Interface Cracks. – Cham: Springer, 2017. – 235 p.
22. *Govorukha V.B., Loboda V.V.* Contact zone models for an interface crack in a piezoelectric material // Acta Mechanica. – 2000. – **140,** N 3. – P. 233 – 246.
23. *Guz A.N.* On Physically Incorrect Results in Fracture Mechanics // Int. Appl. Mech. – 2009. – **45,** N 10. – P. 1041 – 1051.
24. *Herrmann K.P., Loboda V.V.* On interface crack models with contact zones situated in an anisotropic bimaterial // Arch. Appl. Mech. – 1999. – **69,** N 5. – P. 317 – 335.
25. *Herrmann K.P., Loboda V.V.* Fracture-mechanical assessment of electrically permeable interface cracks in piezoelectric bimaterials by consideration of various contact zone models // Arch. Appl. Mech. – 2000. – **70,** N 1. – P. 127 – 143.
26. *Kaminsky A.A., Kipnis L.A., Dudik M.V.* Modeling of the crack tip plastic zone by two slip lines and the order of stress singularity // Int. J. Fract. – 2004. – **127,** N 1. – P. L105 – L109.
27. *Kaminsky A.A., Kurchakov E.E.* Fracture process zone at the tip of a mode I crack in a nonlinear elastic orthotropic material // Int. Appl. Mech. – 2019. – **55,** N 1. – P. 23 – 40.
28. *Kaminsky A.A., Kurchakov E.E.* Mechanism of Development of the Area of Passive Deformation in a Nonlinear Elastic Orthotropic Body with a Crack // Int. Appl. Mech. – 2020. – **56,** N 4. – P. 402 – 414.
29. *Kaminsky A.O.* Studies of Subcritical Crack Growth in Viscoelastic Anisotropic Bodies using the Continued Fraction Operator Method: Synthesis and Summary // Int. Appl. Mech. – 2021. – **57,** N 3. – P. 263 – 281.
30. *Kamins'kyi A.O., Dudyk M.V., Kipnis L.A.* Investigation of the process zone near the tip of an interface crack in the elastic body in shear within the framework of the complex model // J. of Math. Sci. – 2017. – **220,** N 2. – P. 117 – 132.
31. *Kuo A.Y.* Interface Crack Between Two Dissimilar Half Spaces Subjected to a Uniform Heat Flow at Infinity – Open Crack // J. Appl. Mech. – 1990. – **57,** N 2. – P. 359 – 364.
32. *Leguillon D.* Interface crack tip singularity with contact and friction // Comptes Rendus de l'Académie des Sciences – Series IIB – Mechanics – Physics – Astronomy. – 1999. – **327,** N 5. – P. 437 – 442.
33. *Linkov A., Koshelev V.* Multi-wedge points and multi-wedge elements in computational mechanics: evaluation of exponent and angular distribution // Int. J. Solids Struct. – 2006. – **43,** N 18. – P. 5909 – 5930.
34. *Luo Y., Subbarayan G.* A study of multiple singularities in multi-material wedges and their use in analysis of microelectronic interconnect structures // Engng. Fract. Mech. – 2007. – **74,** N 3. – P. 416 – 430.
35. *Pageau S.S., Gadi K.S., Biggers S.B., Joseph P.F.* Standardized complex and logarithmic eigensolutions for n-material wedges and junctions // Int. J. Fract. – 1996. – **77,** N 1. – P. 51 – 76.
36. *Qu J., Bassani J.* Cracks on bimaterial and bicrystal interfaces // J. Mech. Phys. Solids. – 1989. – **37,** N 4. – P. 417 – 433.
37. *Rice J.R., Sih G.C.* Plane problems of cracks in dissimilar media // J. Appl. Mech. – 1965. – **32,** N 2. – P. 418 – 423.
38. *Theocaris P.S., Gdoutos E.E.* Stress singularities in cracked composite full-planes // Int. J. Fract. – 1977. – **13**, N 6. – P. 763 – 773.
39. *Wang S.S., Choi I.* The Interface Crack Between Dissimilar Anisotropic Composite Materials // J. Appl. Mech. – 1983. – **50,** N 1. – P. 169 – 178.
40. *Wieghardt K.* Über das spalten und zerreißen elastischer Körper // Zeitschrift für Mathematik und Physik. – 1907. – **55,** N 1/2. – P. 60 – 103.
41. *Williams M.L.* Stress singularities resulting from various boundary conditions in angular corners of plates in extension // J. Appl. Mech. – 1952. – **19,** N 4. – P. 526 – 528.
42. *Williams M.L.* The stresses around a fault or crack in dissimilar media // Bulletin of the Seismological Soc. of America. – 1959. – **49,** N 2. – P. 199 – 204.
43. *Willis J.R.* The penny-shaped crack on an interface // Quart. J. Mech. Appl. Mathem. – 1972. – **25,** N 3. – P. 367 – 385.

Надійшла 07.10.2021 Затверджена до друку 31.05.2022